Hindawi
Geofluids
Volume 2022, Article ID 5894735, 16 pages
https://doi.org/10.1155/2022/5894735

Research Article

Model of Overlying Strata Structure in Large Mining Height Excavating Condition and Calculation of Support Working Resistance

Fengfeng Wu,[1,2] **Xin Yue**,[1,2] **Jingxuan Yang**,[1,2] **Beiju Du**,[1,2] **Jian Zhang**,[1,2] **and Bo Lv**[1,2]

[1]*Key Laboratory of Deep Coal Resource Mining, Ministry of Education, China University of Mining and Technology, Xuzhou, Jiangsu 221116, China*
[2]*School of Mines, China University of Mining and Technology, Xuzhou, Jiangsu 221116, China*

Correspondence should be addressed to Xin Yue; yuexin@cumt.edu.cn

Received 24 September 2021; Accepted 3 February 2022; Published 15 March 2022

Academic Editor: Hamed Lamei Ramandi

Copyright © 2022 Fengfeng Wu et al. This is an open access article distributed under the Creative Commons Attribution License, which permits unrestricted use, distribution, and reproduction in any medium, provided the original work is properly cited.

Aiming at the wide range of rock strata movement and collapse, poor stability and high damage rate of the working face support and being prone to crushing of the support in large mining height face, analog simulation, theoretical analysis, and field measurements have been carried out to analyze roof breaking structure form and calculation method of support reasonable support resistance of large mining height face. The researches show that, affected by the space of the mined-out area, the roof of the large mining height working face will take on the structural form of "combined suspended beam-nonhinged roof-hinged roof"; the interaction system between the support and the surrounding rock consists of "hinged roof structure," "nonhingeable roof structure," "combined suspension beam structure," and the support. The support resistance should adapt to the change of the overlying rock structure's instability movement, bearing the weight of the structure itself and the additional load generated by the movement. Combining with the mining conditions of Jinhuagong Coal Mine's large mining height face in Datong mining area, the reasonable support resistance of the working face support is analyzed. The mine pressure monitoring shows that the ZZ13000/28/60 type support and shield hydraulic support can meet the requirements of roof control; the research results ensure the safe mining of the large mining height face.

1. Introduction

The thickness of coal strata occurrence in numerous mine areas exceeds 3.5 m in China, i.e., Yanzhou mine areas in Shandong Province, Xishan, Datong, Lu′an, and Jincheng mine areas in Shanxi Province [1–3]. The excavating techniques of thick coal strata, to a large extent, determine the development of technological level of the entire coal mining industry as well as the utilization of economic benefit in China [4–8]. Due to the advantages of high resource recovery and small amount of gas discharge of the excavation of coal strata with large mining height, it has become the main development direction and primary technical approach of the safe and efficient excavation of thick coal strata in Chinese mine areas [9, 10]. In recent years, significant breakthrough had been achieved in the development of associated equipment for the excavation of mine area with large mining height which significantly accelerated the development of excavating techniques for thick coal seam with large mining height [4, 5]. However, years of on-site measurement and abundant theoretical studies showed that, with the increase of excavating depth of the coal strata and the height of support, the stability of the surrounding rock support system weakened and the accident rate exceeded 19% [11, 12]. Common incidents of runover and damage of support occurred due to insufficient working resistance of support at the working face [11]. For example, Jinhuagong Coal Mine is one of the large scale mine areas owned by Datong Coal Mine Group in China which locates at 12.5 km to the west of Datong City. The area of mine is 41 km^2, the

designed production capacity is 4.5 Mt/a, and the average excavating depth of coal strata is 5.7 m. The lithological character of the roofing is mainly sandy strata with high hardness. During the mining period of No. 8218 working face, a total of 3 support crushing incidents occurred and a total period of 21 days of normal production was affected [13].

The existing production practice has confirmed that the overlying strata structure directly relates to the basic problems of stope strata control, such as the causes of stope accidents, the source of roof pressure, the principle of stope support, and the determination of various parameters [14]. Scholars have conducted many studies on the overlying rock structure of working face, which has promoted the solution of the problem of stope roof control. Yan et al. [15] put forward the structure theory of 'short cantilever beam-hinged rock beam' in large mining height stope. Xu et al. [16] put forward the structure theory of 'cantilever beam + masonry beam' in large mining height fully mechanized mining stope. Wang et al. [17] established the structure model of 'cantilever beam + masonry beam' based on the mining conditions of super large mining height working face and analyzed the coupling relationship and control method of strength, stiffness, and stability of hydraulic support and surrounding rock in super large mining height working face. Ju et al. [18] discussed the influence of key strata on the breaking characteristics and working resistance of support in large mining height fully mechanized mining face. Yin [19] put forward the structure model of 'cutting body' for shallow buried large mining height working face. Regarding the calculation of the support load and working resistance of the large mining height face, the traditional empirical formula and engineering analogy methods are still used. Zhang et al. [20] used the position equation method to theoretically analyze the support working resistance of the medium-buried large mining height fully mechanized mining face. Qiu et al. [21] checked the support strength of the shallow buried and large mining height working face through the load empirical formula and the actual measurement statistical method.

However, due to the complexity of the conditions of occurrence as well as the specialty of the excavating techniques for large mining height coal strata, when guided by conventional mining pressure and strata control theory, it is likely that the activity of working face roofing is unclear and the mechanism of mining pressure appearance is unknown, thus hindering the efficient and safe production of the coal mine. Therefore, on the basis of existing research, further analyze the relationship of support and surrounding rocks in large mining height excavating condition through the pattern of fracturing and destabilization overlying strata of working face with large mining height and the structure of the roof structure and thus provide effective and rational roof control techniques, which have great theoretical significance and practical value for the efficient and safe production of coal strata with large mining height.

Based on the engineering background of Jinhuagong Coal Mine, this paper adopts the research methods of physical simulation test, numerical simulation, theoretical analysis, and field measurement to explore the morphology and characteristics of overburden structure in large mining height working face. Based on the results of physical test and numerical analysis, a mechanical model is established to analyze the interaction between support and surrounding rock under this mining condition, and the calculation method of reasonable support resistance under large mining height is deduced to guide the reasonable selection of support and roof control under large mining height. The correctness of the calculation method is verified by engineering practice.

2. Overlying Strata Structure Form of Large Mining Height Mining Face

2.1. Physical Simulation of Overlying Strata Structure

2.1.1. Similarity Model Establishment. In order to evaluate the characteristics of movement and structural mode of overlying rock roofing in large mining height condition, No. 8218 large mining height working face of Jinhuagong Coal Mine was selected as background to conduct physical similar simulation experiment.

2D plane stress experimental station was used to conduct similarity analysis. The size of the experiment model is length × width × height = 2500 × 200 × 2000 mm. The selection of similar analog constants [22] is shown in Table 1. According to similar constants and actual mechanical parameters of coal and rock mass, the physical and mechanical parameters and proportions of the physical model rock formation are calculated, as shown in Table 2. The model is laid in layers along the horizontal direction, and talcum powder and mica powder are sprinkled between the layers. After the model is dry, paint the surface of the model with white ash, and lay vertical and horizontal observation lines on the surface of the model. The intersection of the two lines is used as the observation point. According to the buried depth of the coal seam, the weight of the overlying rock layer is compensated by external force, and the experimental paving model is shown in Figure 1.

2.1.2. Physical Simulation Experiment Results. The results of the experiment are shown in Figure 2. The following can be seen:

(1) During the advancement of 20 m of the working face, the immediate roof fractured in a periodic order and acted directly on the support of the mine area in the mode of combined cantilever beam structure. The overlying rock strata above the immediate roof remained intact. With the increase of distance of advancement, different amount of settlement of the sublayers of the overlying rock strata led to the delamination of the sublayers.

(2) When the working face advanced to 70 m, the collapsed height at the gob increased. The caving gangue gradually filled the space of the gob to support the fractured blocks of the overlying rock strata. However, as the caving gangue was in the initial extrusion

Table 1: Primary similarity constants of similar simulation experiment.

Primary similarity constants	Ratio (model: original)
Geometric similarity ratio	1 : 80
Similarity constant of volumetric weight	1.5
Similarity constant of stress	120
Similarity constant of time	8.9

Table 2: Physical and mechanical parameters of coal strata with large mining height.

Serial number	Lithological characteristics	Paved thickness of the model (cm)	Compressive strength (kPa)	No. of mixture	Sublayer
14	Medium gritstone	4.8	392	455	3
13	Gritstone	6.8	383	455	4
12	Fine sandstone	14.2	450	337	4
11	Coal	1.5	167	764	
10	Sandy shale	6.5	208	546	3
9	Coal	1.2	167	764	
8	Sandy shale	6.5	208	546	3
7	Fine sandstone	2.0	358	455	
6	Sandy shale	3.8	208	546	2
5	Medium sandstone	11.5	392	455	3
4	Gritstone	11.2	358	455	3
3	Fine sandstone	2.9	450	337	
2	Sandy shale	1.1	217	546	
1	Coal	7.1	167	764	

Note. The meaning of No. of mixture: the first digit represents the ratio of sand to cement, and the second and third digits represent the ratio of calcium carbonate to gypsum in the cement. For example, No. 455 of mixture in the table indicates that the sand-to-rubber ratio is 4 : 1, and the calcium carbonate: gypsum in a cement is 5 : 5.

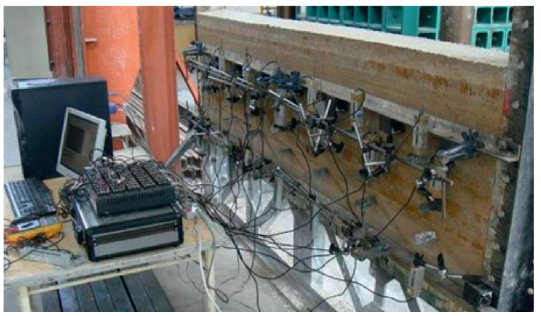

Figure 1: Two-dimensional plane stress test bench.

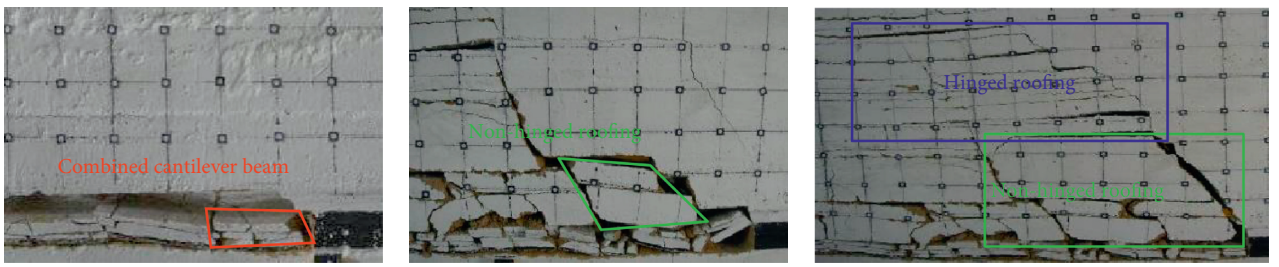

(a) (b) (c)

Figure 2: Damage mode of overlying rock during the advancement of working face. (a) Working face advanced to 20 m; (b) working face advanced to 70 m; (c) working face advanced to 120 m.

stage, the compactness was low and the amount of extrusion was large, the settlement of roofing exceeded the ultimate allowable settlement between the fractured blocks, and thus hinged rock-beam structure could not be formed between the blocks. Instead, nonhinged rock-beam structure existed.

(3) When the working face advanced to 120 m, the space of overlying rock strata reduced and the amount of extrusion of the caving gangue at the gob became limited. The allowable settlement of the fractured roofing was smaller than the ultimate amount of rotation of the overlying rock strata. In addition, large extrusion existed between the fractured blocks. As a result, masonry beam structure was formed between the fractured blocks of the high roofing.

2.2. Numerical Simulation of Breaking Motion Characteristics of Overburden Strata

2.2.1. Numerical Model Establishment. The UDEC2D numerical calculation model is established based on the engineering geological conditions and mining technical conditions of No. 8218 fully mechanized mining face in Jinhuagong Coal Mine.

Model size is height × width = 100 m × 200 m. The constitutive relationship of surrounding rock used in the numerical calculation model is Mohr-Coulomb criterion, stress-displacement mixed boundary, uniform vertical compressive stress is applied to the upper boundary of the model, and horizontal compressive stress varying with depth is applied on both sides. According to the mechanical test data of the coal seams and roof and floor rocks of No. 8218 working face provided by Jinhuagong Coal Mine, the deformation parameters of the coal seams and roof and floor rocks under the Mohr-Coulomb strength criterion are estimated through the GSI geological strength index and the Hoek-Brown strength criterion as shown in Table 3 below.

2.2.2. Numerical Simulation Results. Figure 3 shows the simulation results of the fracture movement characteristics of the overlying strata in the mining process of the working face. It can be seen from the figure that when the working face is at the position of the open cut, the overhang length of the first layer of sandy shale is small and does not reach its limit span. It is a cantilever structure with fixed ends at both ends, as shown in Figure 3(a). As the working face continues to advance, the first and second layered rock formations bend and sink, causing separation from the upper layer. The first and second layered roofs collapsed for the first time, with a collapsed height of 3.2 m, and thickness and hardness of the overlying third layer named coarse sandstone are large, the limit span is large, and the bending deformation of the coarse sandstone is small. As the working face continues to advance, due to the large goaf space at this time, the collapsed first and second layered roof fill the goaf. The height of the zone is limited, and the coarse sandstone roof has a large bending and sinking space. The working face is advanced to 52 m, as shown in Figure 3(b). The coarse sandstone roof collapses and the height of the collapse is 12.2 m. Similarly, due to the large space in the goaf at this time, the collapsed roof rock layer is insufficient to fill the mined-out area, and the allowable sinking space is greater than the limit subsidence of the overlying rock. The overlying rock breaks and collapses and enters the mined-out area. This part of the roof is in the form of a combined cantilever beam above the support. When the working face advances to 66 m, the overlying sandy shale breaks and collapses, filling the mined-out area to a greater degree, and the allowable sinking space is already very small, as shown in Figure 3(c); the roof is in a state of nonarticulated structure. At this time, the collapse height reaches 38.7 m; when the working face advances to 92 m, the overburden fine sandstone collapses for the first time. Because the free space below is filled with falling gangue, the allowable subsidence is less than the thickness of the fine sandstone roof, forming a hinged structure, as shown in Figure 3(d); when the working face advances to 110 m, the fine sandstone roof collapses for the first time, as shown in Figure 3(e); when the working face advances to 130 m, the fine sandstone roof collapses for the second time, as shown in Figure 3(f).

2.3. Structural Features of Overlying Rock Roof in Stope.

Based on the foregoing simulation results, it can be seen that the large mining height working face is affected by the goaf space, and the roof breaking structure of the goaf has the following characteristics:

(1) During the initial mining period of the working face, the immediate roofing existed in the form of combined cantilever beam structure. Affected by the lithological characteristics of the roofing, there is a certain amount of difference in the suspended length of the combined cantilever beam structure. For normal soft roofing, such as mud stone, shale, and sandy shale, the fracturing line lies on the tail beam of the support and the support of the working face mainly carries the weight of the overlying rock. For harder roofing, such as sandstone, limestone, and glutenite, the fracturing line normally lies behind the tail beam of the support by a certain distance and cantilever structure is formed. In this case, apart from sustaining the weight of the collapsed roofing, the support is also subjected to the moment of the cantilever roofing.

(2) The blocks of the nonhinged roofing structure are regularly arranged and there is no compressive action between the blocks. For normal soft roofing, such as mud stone, shale, and sandy shale, the nonhinged roofing structure transforms to combined cantilever beam structure. For harder roofing, such as sandstone, limestone, and glutenite, the fractured dimension of the nonhinged roofing structure is large and the supporting action from the gangue in the gob increases. As a result, the effect on

Table 3: The physical and mechanical property parameters of the numerical simulation experimental model coal.

Serial number	Lithologic characters	Thickness/m	Bulk density (kg/m^3)	Volume modulus (GPa)	Shear modulus (GPa)	Internal friction angle/°	Cohesion (MPa)	Tensile strength (MPa)
15	Grit stone	20.0	2580	8.4	3.72	37	8.27	6.22
14	Fine sandstone	13.4	2580	7.1	2.91	37	5.45	4.06
13	Moderate coarse sandstone	3.8	2580	9.4	6.76	40	6.63	5.27
12	Grit stone	5.4	2580	8.4	3.72	37	8.27	6.22
11	Fine sandstone	11.4	2580	7.1	2.91	37	5.45	4.06
10	Coal seam	1.22	1400	7.22	1.8	28	2.82	3.13
9	Sandy shale	5.22	2420	4.2	2.91	35	4.52	2.47
8	Coal seam	0.96	1400	7.2	1.8	28	2.82	3.13
7	Sandy shale	5.21	2420	4.2	2.91	35	4.52	2.47
6	Fine sandstone	1.60	2580	7.1	2.91	37	5.45	4.06
5	Sandy shale	3.10	2420	4.2	2.91	35	4.52	2.47
4	Medium sandstone	9.20	2580	9.6	4.7	32	7.20	5.21
3	Grit stone	9.00	2580	8.4	3.72	37	8.27	6.22
2	Fine sandstone	2.30	2580	7.1	2.91	37	5.45	4.06
1	Sandy shale	0.90	2420	4.2	2.91	35	4.52	2.47
	Coal seam	5.70	1400	7.2	1.8	28	2.82	3.13

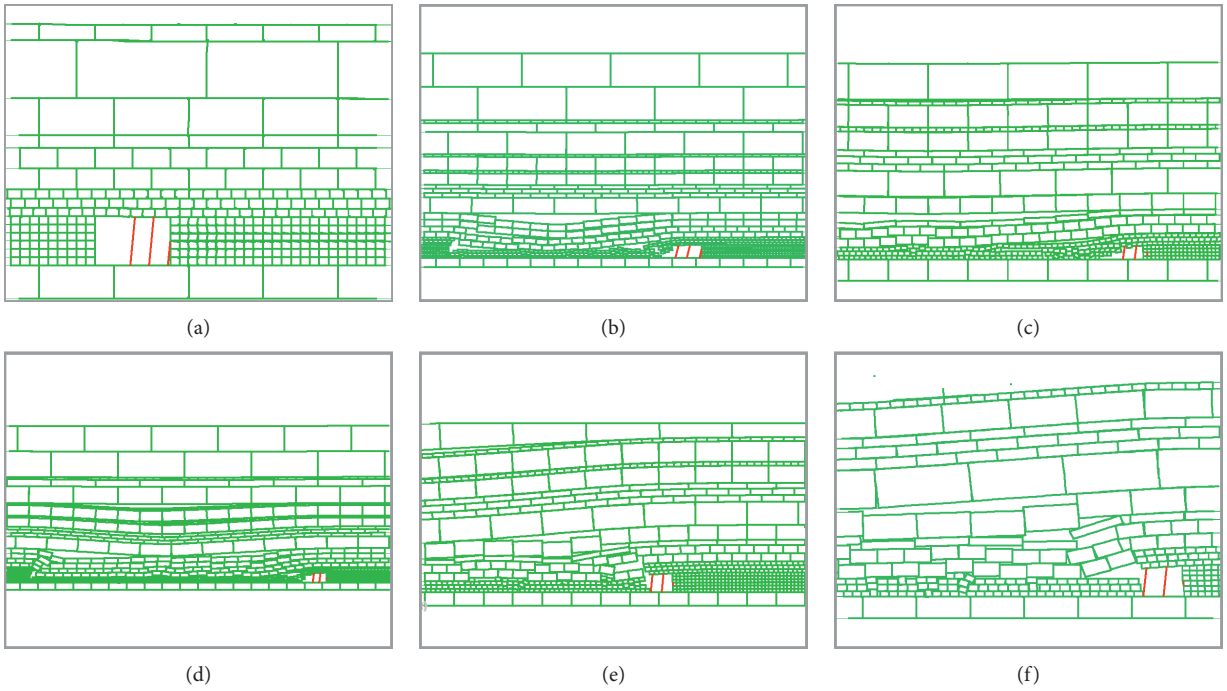

Figure 3: Numerical simulation of overburden failure mode. (a) Open-off cut position; (b) working face advanced to 52 (m); (c) working face advanced to 66 (m); (d) working face advanced to 92 (m); (e) first periodic collapse of basic roof; (f) second periodic collapse of basic roof.

the underneath combined cantilever beam structure is reduced.

(3) When the hard rock strata above the nonhinged roofing fracture, the allowable settlement is limited and the fractured blocks form hinged roofing structure due to mutual extrusion. Unconnected fracturing appears on the overlying roofing and the roofing is primarily subjected to bending settlement.

The "combined cantilever structure-nonhinged roof structure-hinged roof structure" model of the overlying rock roof of the large mining height working face is shown in Figure 4.

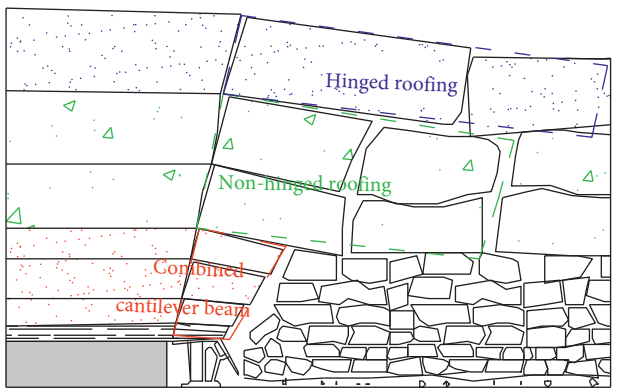

Figure 4: Roof structure model of large mining height working face.

3. Relationship between Support and Surrounding Rock and Calculation of Support Resistance

With the increase of mining height, the failure range of overlying strata and the degree of motion instability increase, which will cause the increase of mining pressure. Therefore, under the condition of fully mechanized mining with large mining height, the interaction between support and surrounding rock is the key problem related to the influence of roof breaking and instability on support and the determination of reasonable working resistance of support.

According to the above analysis, after ignoring the influence of the floor, the interaction system of the surrounding rock of the support in the fully mechanized mining face with large mining height is composed of the support-combined cantilever beam structure-nonhinged roof structure-hinged roof structure, as shown in Figure 5.

The working state and supporting quality of the support affect the stability of the combined cantilever beam structure and the nonhinged roof structure, and the stability of the latter two in turn affects the support. As the external condition of the support, the combined cantilever beam structure and the nonhinged roof structure system, the hinged roof structure has a significant impact on its stability. Due to the existence of the influence angle of the coal wall support in the stope and the fact of the continuous advancement of the working face, the rotation of the hinged roof structure is uncontrollable. Therefore, the motion and action of the hinged roof are dominant in the interaction system of the surrounding rock of the support.

This structural model is derived under the condition of the hard roof of Jinhuagong Coal Mine. The overburden structure is also the form of expression under the most difficult conditions of rock formation control in the large mining height face, and it describes the temporal and spatial characteristics of the overburden movement instability in the large mining height and large mining space. However, as analyzed above, with the change of the lithological conditions of the overlying rock roof, the structure of the overlying rock will also change. For example, when the direct roof lithology is weak rock formations such as mudstone and shale, the lower composite cantilever structure will not exist, and when the thickness of the weak direct roof rock layer is very thick, the nonhinged roof will also not exist. Therefore, the structural characteristics of the thick coal seam and large mining height overlying rock should be analyzed in detail according to the specific conditions of the overlying rock. To sum up, this structural model is also a general model of overlying strata structure in large mining height stopes in thick coal seams.

3.1. Interaction between Roof Combined Cantilever Beam Structure and Support. Before the breaking and instability of the key strata above, the support of the working face mainly bears the structural action of the combined cantilever beam of the direct roof strata. The stress model of the support of the working face and the combined cantilever beam of the direct roof strata in the coal seam with large mining height is shown in Figure 6.

In Figure 6, P_Z is the support resistance of working face, and c is the distance between the support resistance action point and the roof fracture line position (generally located in the coal wall position). $H_{11} \sim h_{1k}$ are the layered thickness of combined cantilever beam structure, respectively. α_{11}~α_{1k} are the layered fracture angles of the combined cantilever beam roof, respectively. k is the total number of combined cantilever rock strata. P_{11}~P_{1k} are the layered weight of combined cantilever beam structure, respectively. l_{11}~l_{1k} are the layered fracture sizes of combined cantilever beam structure, respectively. R_x is the force of overlying rock above combined cantilever beam on combined cantilever beam structure. l_x is the distance between overburden force above combined cantilever beam and roof fracture line.

Taking the moment of O point in the graph, the equilibrium conditions of the immediate roof combined cantilever beam structure are calculated as follows:

$$P_z c \geq \frac{1}{2} P_{11} \left(h_{11} \cot \alpha_{11} + l_{11}\right) + P_{12}\left(\frac{1}{2} h_{12} \cot \alpha_{12} + \frac{1}{2} l_{12} + h_{11} \cot \alpha_{11}\right) + \cdots + P_{1k}\left(\frac{1}{2} h_{1k} \cot \alpha_{1k} + \frac{1}{2} l_{1k} + \sum_{i=1}^{k-1} h_{1i} \cot \alpha_{1i}\right) + R_x\left(l_x + \sum_{i=1}^{k} h_{1i} \cot \alpha_{1i}\right). \quad (1)$$

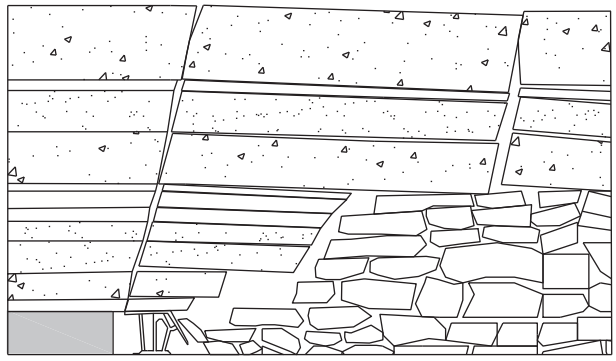

Figure 5: The relationship between support surrounding rock of fully mechanized working face with large mining height.

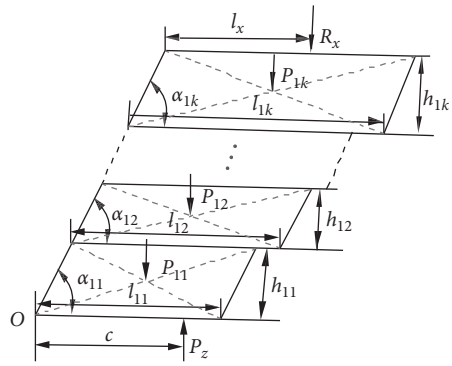

Figure 6: Roof combined cantilever beam structural model.

Among them: h_{1i} is the i layer thickness of combined cantilever beam roof, while i is the sequence number of layered roof.

After the consolidation of formula (1), the stability condition of the combined cantilever beam roof structure in coal seam with large mining height is obtained as follows:

$$P_z c \geq \frac{1}{2}\sum_{i=1}^{k} P_{1i}\left(h_{1i}\cot\alpha_{1i} + l_{1i}\right) + \sum_{j=2}^{k}\sum_{i=1}^{j-1} P_{1j}h_{1i}\cot\alpha_{1i} + R_x\left(l_x + \sum_{i=1}^{k} h_{1i}\cot\alpha_{1i}\right). \tag{2}$$

It can be seen from formula (2) that the stability conditions of the roof combined cantilever beam structure are not only related to the weight, thickness, fracture angle, roof fracture size, and the bearing capacity of the working face support itself and the position of the action point of the multilayer roof of the cantilever beam structure, but also affected by the indirect force of the overlying strata of the combined cantilever beam structure and the position of the action point.

Before the overlying strata of the roof combined cantilever beam structure are unstable and broken, the force of the complete roof structure of the overlying strata on the broken roof combined cantilever beam structure can be ignored, namely, $R_x = 0$.

According to formula (2), the support resistance under the critical instability condition of the roof combined cantilever beam structure in the working face of large mining height coal seam can be determined as

$$P_z = \frac{1}{2c}\left[\sum_{i=1}^{k} P_{1i}\left(h_{1i}\cot\alpha_{1i} + l_{1i}\right) + 2\sum_{j=2}^{k}\sum_{i=1}^{j-1} P_{1j}h_{1i}\cot\alpha_{1i}\right]. \tag{3}$$

By formula (3), the support resistance of the combined cantilever beam roof structure of the working face in the large mining height coal seam mainly depends on the weight, thickness, fracture angle, roof fracture size, and the position of the working face support resistance.

When the roof fracture angle takes a certain value, the relationship between the support resistance and the position of the support action point is shown in Figure 7.

It can be seen from Figure 6 that, under certain roof fracture angle, the support resistance of the working face decreases with the increase of the distance between the position of the support action point and the roof fracture line, which is easy to understand from the perspective of the torque balance of the roof combined cantilever beam structure. It can also be seen that the support resistance of the working face tends to decrease with the increase of the roof fracture angle, but with the increase of the position distance of the support action point, the variation gradient of the support resistance of the working face increases with the increase of the roof fracture angle.

3.2. Interaction between Roof Nonhinged Structure and Combined Cantilever Beam Structure. The stress characteristics of nonhinged roof structure are shown in Figure 8.

From Figure 8, it can be seen that the nonhinged roof structure is not only affected by the weight of its own rock strata and overburden load, but also supported by the cantilever beam structure from the lower roof and the caving gangue in the goaf. At this time, the roof structure maintains balance and stability under the synergy of various forces. The O point moment of the nonhinged roof composite structure is taken, and the mechanical equilibrium conditions of the roof structure are obtained as follows:

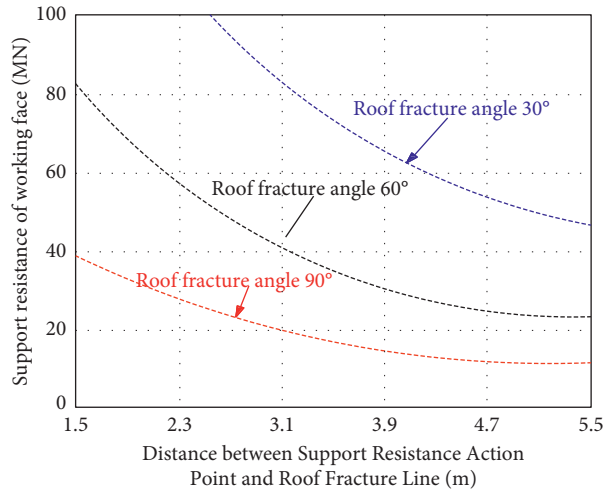

Figure 7: The relationship between support resistance and point action.

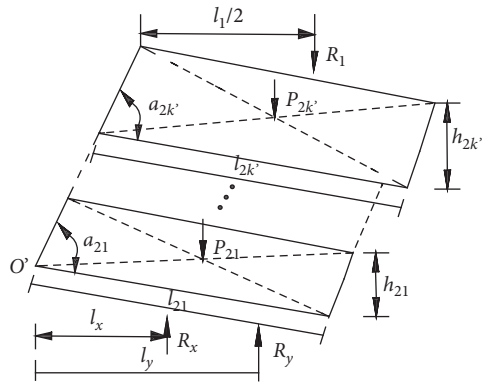

Figure 8: The model of nonhinged roof structure.

$$R_x l_x + R_y l_y \geq \frac{1}{2} P_{21}\left(h_{21}\cot\alpha_{21} + l_{21}\right) + P_{22}\left(\frac{1}{2}h_{22}\cot\alpha_{22} + \frac{1}{2}l_{22} + h_{21}\cot\alpha_{21}\right) + \cdots + P_{2k'}\left(\frac{1}{2}h_{2k'}\cot\alpha_{2k'} + \frac{1}{2}l_{2k'} + \sum_{i=1}^{k'-1} h_{2i}\cot\alpha_{2i}\right) + R_1\left(\frac{1}{2}l_1 + \sum_{i=1}^{k'} h_{2i}\cot\alpha_{2i}\right). \tag{4}$$

Among them: R_x and R_y are the force of the lower combined cantilever beam and the goaf caving gangue on the overlying nonhinged roof structure. l_x and l_y are the distance between the forces R_x, R_y and O′ point. R_1 and l_1 are the force and position of action point of overlying strata on nonhinged roof structure. k' is the total number of nonhinged roof layers. P_{2i}, l_{2i}, h_{2i}, and α_{2i} are the weight, length, thickness, and fracture angle of the i-stratification of nonhinged roof structure; i value is $1\sim k'$.

After combining formula (4), the stability condition of nonhinged roof structure is obtained as follows:

$$R_x l_x + R_y l_y \geq \frac{1}{2}\sum_{i=1}^{k'} P_{2i}\left(h_{2i}\cot\alpha_{2i} + l_{2i}\right) + \sum_{j=2}^{k'}\sum_{i=1}^{j-1} P_{2j}h_{2i}\cot\alpha_{2i} + R_1\left(\frac{l_1}{2} + \sum_{i=1}^{k'} h_{2i}\cot\alpha_{2i}\right). \tag{5}$$

It can be seen from formula (5) that the load from the overlying rock of the roof structure and the weight of the structure itself maintain a certain balance under the combined action of the lower combined cantilever beam structure and the falling gangue in the goaf. Under certain roof overburden load conditions, there is an inverse

correlation between the force of the combined cantilever beam structure on the working face and the support force of the gangue in the goaf. Improving the support effect of the gangue in the goaf will play a positive role in reducing the force of the combined cantilever beam structure.

From formula (5), the bearing relationship of roof combined cantilever beam structure and goaf caving gangue on overlying nonhinged roof structure is satisfied:

$$R_x l_x + R_y l_y = \frac{1}{2}\sum_{i=1}^{k'} P_{2i}\left(h_{2i}\cot\alpha_{2i} + l_{2i}\right) + \sum_{j=2}^{k'}\sum_{i=1}^{j-1} P_{2j}h_{2i}\cot\alpha_{2i}. \tag{6}$$

Combined with goaf gangue support force calculation formula (7):

$$R_y = \lambda\sum_{i=1}^{k'} P_{2i}. \tag{7}$$

According to the stability condition of roof combined cantilever beam shown in formula (2), the support resistance of working face under the critical instability condition of nonhinged roof structure is

$$P_z = \frac{\left[(1/2)\sum_{i=1}^{k} P_{1i}\left(h_{1i}\cot\alpha_{1i} + l_{1i}\right) + \sum_{j=2}^{k}\sum_{i=1}^{j-1} P_{1j}h_{1i}\cot\alpha_{1i} + R_x\left(l_x + \sum_{i=1}^{k} h_{1i}\cot\alpha_{1i}\right)\right]}{c}. \tag{8}$$

The stress characteristics of 'working face support-goaf gangue-roof combined cantilever beam structure-roof nonhinged structure' are shown in Figure 9.

The working face support is stable under the combined action of overburden roof weight and goaf gangue. Combining formula (2) and formula (5), the support resistance under the action of nonhinged roof structure is calculated as

$$P_z = \frac{\left(G_1 + G_2 + G_3\right)}{c}. \tag{9}$$

Among them:

$$\begin{aligned} G_1 &= \frac{1}{2}\left[\sum_{i=1}^{k} P_{1i}\left(h_{1i}\cot\alpha_{1i} + l_{1i}\right) + \sum_{i=1}^{k'} P_{2i}\left(h_{2i}\cot\alpha_{2i} + l_{2i}\right)\right], \\ G_2 &= \sum_{j=2}^{k}\sum_{i=1}^{j-1} P_{1j}h_{1i}\cot\alpha_{1i} + \sum_{j=2}^{k'}\sum_{i=1}^{j-1} P_{2j}h_{2i}\cot\alpha_{2i}, \\ G_3 &= \frac{1}{l_x}\left[\frac{1}{2}\sum_{i=1}^{k'} P_{2i}\left(h_{2i}\cot\alpha_{2i} + l_{2i}\right) + \sum_{j=2}^{k'}\sum_{i=1}^{j-1} P_{2j}h_{2i}\cot\alpha_{2i} - R_y l_y\right]\left(\sum_{i=1}^{k} h_{1i}\cot\alpha_{1i}\right) - R_y l_y. \end{aligned} \tag{10}$$

Among them: $G1$, $G2$, and $G3$ are the working resistance components related to the weight of overburden roof, the relevant geometric dimensions, the gangue force in goaf, and the position of action point, respectively.

3.3. Interaction between Roof Articulated Structure and Nonarticulated Structure. Considering that the allowable deflection space of overlying rock at the layer position of hinged roof structure is limited, and the force distribution between the roof layers is relatively uniform, the force between the hinged roof layers is simplified as the concentrated load acting on the middle of the layered fracture block, and the mechanical model is established with two key rock blocks as the research objects, as shown in Figure 10.

In the figure, P_1 and P_2 are the loads (including self-weight) borne by the block. θ_1 and θ_2 are the rotation angles of two adjacent blocks, respectively. w_1 and w_2 are the subsidence of the two blocks, respectively. Q_A and Q_C are the friction forces on the block contact surface. R_1 and R_2 are the support forces of the two blocks under the lower rock stratum, respectively. l_1 and l_2 are the fracture lengths of the two blocks, respectively. T is the horizontal thrust between block structures.

The geometric relations of the block structure in the process of motion are satisfied:

$$\begin{aligned} w_1 &= l_1\sin\theta_1, \\ w_2 &= l_1\sin\theta_1 + l_2\sin\theta_2, \\ a_1 &= \frac{1}{2}\left(h - l_1\sin\theta_1\right), \\ a_2 &= \frac{1}{2}\left(h - l_2\sin\theta_2\right). \end{aligned} \tag{11}$$

Among them: h is the thickness of broken roof strata. a_1 and a_2 are the length of the extrusion contact surface

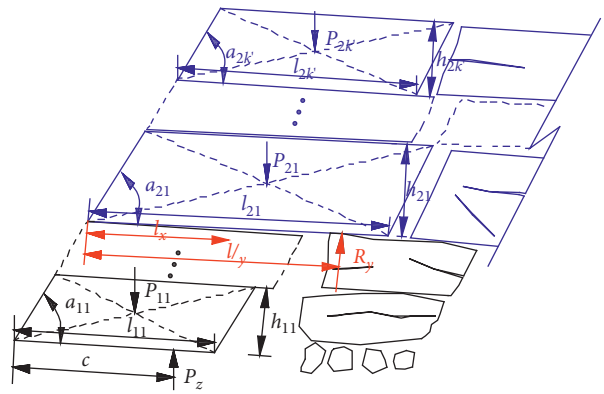

Figure 9: Nonhinged roof structure of bearing system under stress.

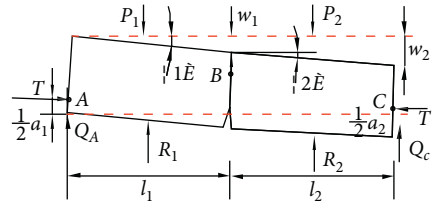

Figure 10: The movement structure and force of two key blocks.

between the two blocks, respectively. Since the contact between the broken blocks under strong extrusion force is a plastic hinge relationship, it is assumed that the position of the action point of the horizontal thrust is half of the length of the extrusion contact surface.

The hinged roof structure is in equilibrium under the combined action of surrounding rock load. According to the equilibrium conditions in the vertical direction of the structure:

$$P_1 + P_2 = Q_A + R_1 + R_2 + Q_c. \tag{12}$$

According to the moment equilibrium conditions $\sum M_A = 0$ and $\sum M_B = 0$ at A and B points in the graph, the following results are obtained:

$$\frac{1}{2}Ta_1 + \frac{1}{2}P_1 l_1 + P_2\left(l_1 + \frac{1}{2}l_2\right) - T\left(\frac{1}{2}a_2 - w_2\right) - Q_c(l_1 + l_2) - R_2\left(l_1 + \frac{1}{2}l_2\right) - R_1 l_1 = 0, \tag{13}$$

$$\frac{1}{2}P_2 l_2 + T(w_2 - w_1 + h - a_2) - Q_c l_2 - \frac{1}{2}R_2 l_2 = 0. \tag{14}$$

For ease of description, $i_1 = h/l_1$ and $i_2 = h/l_2$ are set here to reflect the block size of the broken block. The smaller the value is, the larger the length of the broken block is. Combining formulas (13) and (14), the extrusion force between the broken blocks and the friction force on the extrusion surface are calculated as follows:

$$\begin{cases} T = \dfrac{2(P_1 - 2R_1 + P_2 - R_2)}{2(i_1 + i_2) + (6 + i_1/i_2)\sin\theta_2 - 3\sin\theta_1}, \\ Q_c = \dfrac{(P_1 - 2R_1 + P_2 - R_2)(3\sin\theta_2 + i_2)}{2(i_1 + i_2) + (6 + i_1/i_2)\sin\theta_2 - 3\sin\theta_1} + \dfrac{1}{2}(P_2 - R_2), \\ Q_A = P_1 - R_1 + \dfrac{1}{2}(P_2 - R_2) - \dfrac{(P_1 - 2R_1 + P_2 - R_2)(3\sin\theta_2 + i_2)}{2(i_1 + i_2) + (6 + i_1/i_2)\sin\theta_2 - 3\sin\theta_1}. \end{cases} \tag{15}$$

It can be seen from the calculation of the whole structure of the masonry beam that $R_2 = 1.03P_2$, and because the right block is clamped by the overlying rock roof and the falling gangue in the goaf, the stress characteristics in the vertical direction of the block can be approximately expressed as $R_2 = P_2$. In the process of coal seam mining, the roof periodic breaking, due to the change of roof occurrence conditions, is small; the roof periodic breaking step distance is basically the same, so here take $l_1 = l_2$; the stress characteristics of hinged block of overburden roof are

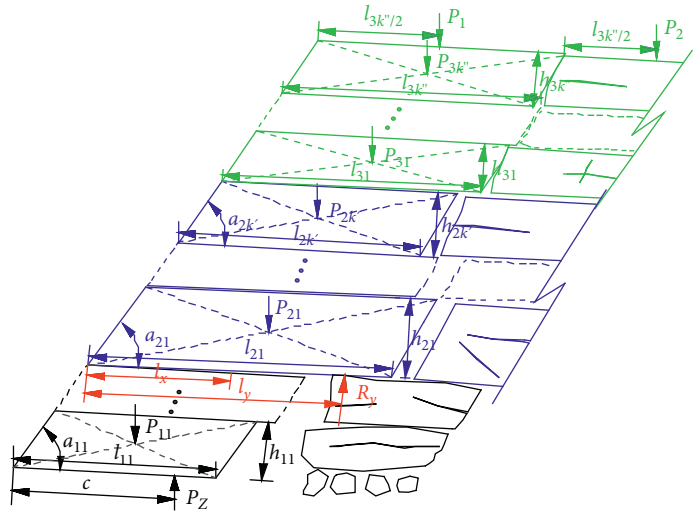

Figure 11: Rock movement characteristics under the hinged roof structure.

$$T = \frac{2(P_1 - 2R_1)}{4i + 7\ \sin\theta_2 - 3\ \sin\theta_1}, \tag{16}$$

$$Q_c = \frac{(P_1 - 2R_1)(3\ \sin\theta_2 + i)}{4i + 7\ \sin\theta_2 - 3\ \sin\theta_1}, \tag{17}$$

$$Q_A = P_1 - R_1 - \frac{(P_1 - 2R_1)(3\ \sin\theta_2 + i)}{4i + 7\ \sin\theta_2 - 3\ \sin\theta_1}. \tag{18}$$

Among them, $i = i_1 = i_2$.

The mechanical characteristics of the bearing system of 'working face support-goaf caving gangue-roof composite suspension beam-nonarticulated roof-articulated roof' are shown in Figure 11.

The discussion of roof nonhinged structure and combined cantilever beam structure has been discussed in the previous paper, so this paper focuses on the analysis of overburden hinged roof structure. The roof hinged structure maintains balance and stability under the weight of overlying strata, surrounding rock support, and extrusion force. The structural stress characteristics are shown in Figure 12.

In the figure, R_1 is the force of the lower nonhinged roof structure on the hinged roof. k'' is the total number of layers of hinged roof. P_{3i}, l_{3i}, h_{3i}, and α_{3i} are the weight, length, thickness, and fracture angle of the i-stratification roof of hinged roof structure; i value is $1 \sim k''$. $Q_A\ k''$ and $Q_B\ k''$ are the friction forces on the extrusion surface of the hinged roof breaking block, respectively. $T_3\ k''$ is the extrusion force on the extrusion surface of the broken block.

Similarly, according to the moment equilibrium condition of the hinged roof structure, the calculation results are as follows:

$$\begin{aligned}&\frac{1}{2}\sum_{i=1}^{k'} T_{3i}a_{3i} + \sum_{j=2}^{k'}\sum_{i=1}^{j-1} T_{3j}h_{3i} - \sum_{j=2}^{k'}\sum_{i=1}^{j-1} Q_{Aj}h_{3i}\cot\alpha_{3i} + P_1\left(\frac{l_{3k'}}{2} + \sum_{i=1}^{k'} h_{3i}\cot\alpha_{3i}\right) + \frac{1}{2}\sum_{i=1}^{k'} P_{3i}h_{3i}\cot\alpha_{3i}\\ &+\frac{1}{2}\sum_{i=1}^{k'} P_{3i}l_{3i} + \sum_{j=2}^{k'}\sum_{i=1}^{j-1} P_{3j}h_{3i}\cot\alpha_{3i} - \sum_{j=2}^{k'}\sum_{i=1}^{j-1} Q_{Bj}h_{3i}\cot\alpha_{3i} - \sum_{i=1}^{k'} Q_{Bi}l_{3i} - \sum_{j=1}^{k'}\sum_{i=1}^{j} T_{3j}h_{3i} + \sum_{i=1}^{k'} T_{3i}w_{3i} + \frac{1}{2}\sum_{i=1}^{k'} T_{3i}a_{3i} - \frac{1}{2}R_1 l_{31} = 0.\end{aligned} \tag{19}$$

The force of the roof hinge structure on the lower strata is

$$R_1 = \frac{\left\{\sum_{i=1}^{k}\left[2T_{3i}(a_{3i} - h_{3i} + w_{3i}) + (P_{3i} + 2P_1)h_{3i}\cot\alpha_{3i} + (P_{3i} - 2Q_{Bi})l_{3i}\right] + 2\sum_{j=2}\sum_{i=1}^{j-1}\left(P_{3j} - Q_{Aj} - Q_{Bj}\right)h_{3i}\cot\alpha_{3i} + P_1 l_{3k'}\right\}}{l_{31}}. \tag{20}$$

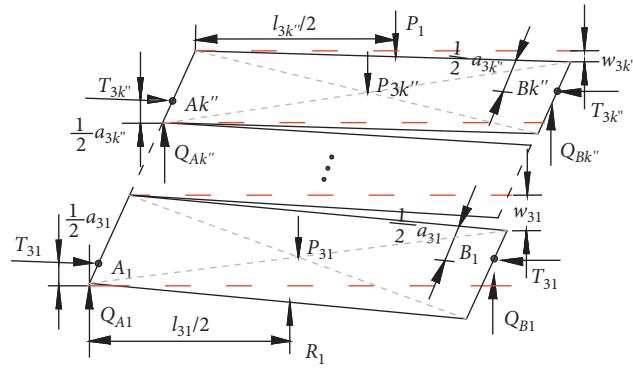

Figure 12: The force characteristic of hinged roof structure.

3.4. Determination of Working Resistance of Support in Working Face. The stress of stope support comes from the effect of direct roof weight and basic roof movement on support. The overlying strata structure of support in fully mechanized mining face with large mining height is composed of hinged roof structure, nonhinged roof structure, and combined cantilever beam structure. The instability movement of a certain structure will have an impact on the support of working face, which is reflected in the strata behavior of working face, mainly the change of support working resistance. Therefore, the support resistance should be able to adapt to the change of instability movement of overburden structure, bearing the weight of structure itself and the additional load generated by movement. Based on the analysis of the previous sections and formulas (2), (5), and (18), the calculation formula of working resistance of working face support is

$$P_z = p_1 + p_2 + p_3 + p_4. \tag{21}$$

Among them:

$$\begin{aligned}
p_1 &= \frac{(1/2)\sum_{i=1}^{k} P_{1i}\left(h_{1i}\cot\alpha_{1i} + l_{1i}\right) + \sum_{j=2}^{k}\sum_{i=1}^{j-1} P_{1j}h_{1i}\cot\alpha_{1i} + \sum_{j=2}^{k'}\sum_{i=1}^{j-1} P_{2j}h_{2i}\cot\alpha_{2i} + (1/2)\sum_{i=1}^{k'} P_{2i}\left(h_{2i}\cot\alpha_{2i} + l_{2i}\right) - R_y l_y}{c},\\
p_2 &= \frac{1}{cl_{31}}\left(\frac{l_{31}}{2} + \sum_{i=1}^{k'} h_{2i}\cot\alpha_{2i}\right)\left\{2\sum_{j=2}^{k''}\sum_{i=1}^{j-1}\left(P_{3j} - Q_{Aj} - Q_{Bj}\right)h_{3i}\cot\alpha_{3i} + P_1 l_{3k''} + \sum_{i=1}^{k''}\left[2T_{3i}\left(a_{3i} - h_{3i} + w_{3i}\right) + \left(P_{3i} + 2P_1\right)h_{3i}\cot\alpha_{3i}\right.\right.\\
&\quad \left.\left. + \left(P_{3i} - 2Q_{Bi}\right)l_{3i}\right]\right\},\\
p_3 &= \frac{1}{cl_x}\left[\frac{1}{2}\sum_{i=1}^{k'} P_{2i}\left(h_{2i}\cot\alpha_{2i} + l_{2i}\right) + \sum_{j=2}^{k'}\sum_{i=1}^{j-1} P_{2j}h_{2i}\cot\alpha_{2i} - R_y l_y\right]\sum_{i=1}^{k} h_{1i}\cot\alpha_{1i},\\
p_4 &= \frac{1}{cl_{31}l_x}\left[\left(\frac{l_{31}}{2} + \sum_{i=1}^{k'} h_{2i}\cot\alpha_{2i}\right)\sum_{i=1}^{k} h_{1i}\cot\alpha_{1i}\right]\left\{2\sum_{j=2}^{k''}\sum_{i=1}^{j-1}\left(P_{3j} - Q_{Aj} - Q_{Bj}\right)h_{3i}\cot\alpha_{3i} + P_1 l_{3k''}\right.\\
&\quad \left. + \sum_{i=1}^{k''}\left[2T_{3i}\left(a_{3i} - h_{3i} + w_{3i}\right) + \left(P_{3i} + 2P_1\right)h_{3i}\cot\alpha_{3i} + \left(P_{3i} - 2Q_{Bi}\right)l_{3i}\right]\right\}.
\end{aligned} \tag{22}$$

Among them: $p_1 \sim p_4$ are the support resistance components of working face under articulated roof structure.

It can be seen that p_1 is mainly the component of support resistance caused by the combined cantilever beam of overlying strata, the weight of rock strata of nonhinged roof structure, and the support effect of gangue in goaf, p_2 is mainly the resistance component caused by the weight of hinged roof strata and the interaction between hinged broken blocks, p_3 is mainly caused by the nonhinged roof structure and the additional effect of goaf caving gangue, and p_4 mainly comes from the additional effect during the movement of hinged roof breaking block.

4. Case Analysis

4.1. Determination of the Working Resistance of the Support. Based on the mining conditions of No. 8218 large mining height coal seam face of Jinhuagong Coal Mine, combined with the research on the interaction relationship between the

abovementioned overlying rock structure and the support, the characteristics of the overlying rock structure of the coal roof are analyzed, and the support resistance of the working face is calculated. To provide reference for analyzing the appearance and mechanism of rock pressure on working face:

(1) Firstly, analyze the force of the combined cantilever structure on the support of the working face under the action of the combined cantilever beam structure. The height of the roof composite cantilever beam structure is about 26.1 m. It can be determined that the roof composite cantilever beam structure under the coal seam mining conditions of Jinhuagong Coal Mine is composed of the first to sixth layered roofs above the coal seam. The physical and mechanical characteristics of the roof composite cantilever structure rock are shown in Table 4.

Substituting the relevant data in Table 4 into formula (3), the change characteristics of the support resistance of the working face with the roof fracture angle are obtained, as shown in Figure 13.

Results that have been achieved have shown that the fracture angle of sandstone roofs is generally 85~90°, and the fracture angle in the physical simulation is 85°. Therefore, according to the conditions of Jinhuagong Coal Mine and the physical simulation test, the fracture angle of 85° is selected for the calculation of the working resistance. The other parameters are shown in Table 4. Only the role of the combined cantilever structure is considered, and the support resistance of the working face is about 12 MN.

(2) The nonhinged roof structure of No. 8218 high mining height coal seam is composed of the 7th~10th roof stratification of the overlying rock, and its physical and mechanical characteristics are shown in Table 5.

The relevant data in Table 5 are substituted into formula (5). If the hinged structure of the overlying rock roof is stable, and the fracture angle of the nonhinged roof is 85 ~ 90°, the support resistance of No. 8218 working face with large mining height should be between 12 and 13 MN when the combined cantilever beam and the nonhinged roof structure are considered.

(3) Finally, the stress of working face support under the action of articulated roof structure is analyzed. The hinged roof structure of working face is the masonry beam structure after the broken roof of No. 11 fine medium coarse sandstone, and its physical and mechanical characteristics are shown in Table 6.

The relevant data is substituted into formula (18) to calculate the force on the lower strata when the hinged roof structure is stable:

$$R_1 = T_{31}(\sin\theta_1 - i_{31}) + (P_{31} + 2P_1)i_{31}\cot\alpha_{31} + (P_{31} - 2Q_{B1} + P_1). \quad (23)$$

According to formulas (16)~(18) and the equilibrium condition in the vertical direction of the rock stratum, the extrusion force between the broken blocks of the hinged roof and the friction force on the extrusion contact surface are calculated as follows:

$$T_{31} = \frac{2(P_1 + P_{31} - 2R_1)}{4i_{31} + 7\sin\theta_2 - 3\sin\theta_1}, \quad (24)$$

$$Q_{B1} = P_{31} + \frac{(P_1 - 2R_1)(3\sin\theta_2 + i_{31})}{4i_{31} + 7\sin\theta_2 - 3\sin\theta_1}. \quad (25)$$

Among them, $i_{31} = h_{31}/l_{31}$.

Combined with the above calculation results, the support resistance of No. 8218 fully mechanized working face with large mining height should be between 13 and 15 MN. Therefore, the reasonable support working resistance of No. 8218 large mining height working face in Jinhuagong Coal Mine should not be less than 15 MN.

4.2. Working Face Support Selection. No. 8210 fully mechanized mining face with large mining height is the second large mining height working face in mine mining. Its position is the same as No. 8218 large mining height working face in No. 402 panel of 12 # coal seam, and the same coal seam is mined. In order to prevent similar crushing accidents in No. 8210 large mining height working face, and taking into account the existing equipment in the mining area, the ZZ13000/28/60 hydraulic support produced by Shanxi Pingyang Heavy Industry Machinery Co., Ltd., is selected in No. 8210 working face. The main technical parameters, as shown in Table 7, are supplemented by advanced blasting presplitting roof control technology measures to control the roof.

4.3. The Measured Analysis of Strata Behaviors. The ground pressure behavior of No. 8210 working face with large mining height was measured on-site. The automatic pressure recorder of Youluoka fully mechanized coal mining was used to continuously record the pressure behavior of the support in the working face. According to the difference of strata behaviors in the inclined direction of the working face, the working face is divided into three measuring areas. Five measuring lines are arranged at the positions of 25 #, 40 #, 55 #, 70 #, and 80 # supports in the central measuring area, and one measuring line is arranged at the positions of 10 # and 89 # supports at both ends, as shown in Figure 14.

The measured results show that the average end resistance of the support in the working face is 8731 kN, accounting for 67.2% of the rated working resistance of the support (13000 kN). During roof weighting, the maximum working resistance of working face support is 12611 kN, accounting for 97.0% of the rated working resistance of support. The average time-weighted working resistance of the support is 8540 kN, accounting for 65.7% of the rated working resistance of the support, and the maximum value is 11186 kN. The maximum time-weighted resistance is about 86.1% of the rated resistance of the support in the working

Table 4: The physical and mechanical characteristics of the roof combination of cantilever structure of No. 8218 large mining height working face.

Serial number	Lithology	Density kg/m^3	Thickness (m)	Tensile strength (MPa)	Top plate force (MPa)	Breaking step (m)	Weight of broken block (MN)
6	Fine sandstone	2438	1.60	4.06	0.09	4.90	1.21
5	Sandy shale	1426	3.10	2.47	0.11	1.56	0.32
4	Medium sandstone	2453	9.20	5.21	0.22	3.80	1.66
3	Coarse sandstone	2683	9.00	6.22	0.44	15.47	3.40
2	Fine sandstone	2645	2.30	4.06	0.59	8.88	1.34
1	Sandy shale	2468	0.90	2.47	0.05	3.43	0.16
	Coal seam	1476	4.14				

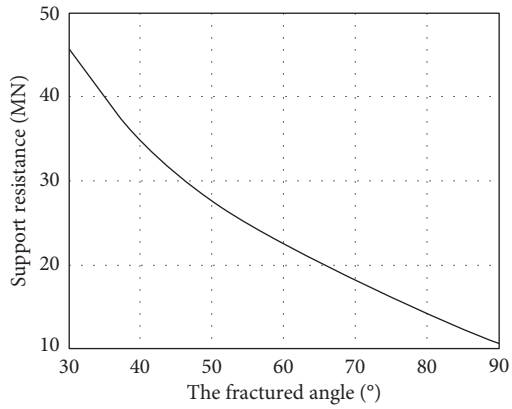

Figure 13: The relationship of stent resistance and the roof fracture angle of combination cantilever ($c = 5.5$ m).

Table 5: The physical and mechanical characteristics of the nonhinged roof structure of No. 8218 large mining height working face.

Serial number	Lithologic characters	Density kg/m^3	Thickness (m)	Tensile strength (MPa)	Roof stress (MPa)	Break step (m)	Broken block weight (MN)
0	Coal seam	1423	1.22	3.13	0.01	3.45	0.30
9	Sandy shale	2514	5.22	2.47	0.19	17.11	5.79
8	Coal seam	1423	0.96	3.13	0.24	30.89	7.42
7	Sandy shale	2514	5.21	2.47	0.19	17.11	5.79

Table 6: The physical and mechanical characteristics of the hinged roof structure of No. 8218 large mining height working face.

Serial number	Lithologic characters	Density kg/m^3	Thickness (m)	Antitension degree (MPa)	Roof by force (MPa)	Breaking step distance (m)	Broken blocks weight (MN)
13	Moderate coarse sandstone	2685	3.8	5.27	0.26	20.86	
12	Grit stone	2647	5.4	6.22	0.40	23.64	
11	Fine sandstone	2732	11.4	4.06	0.68	36.93	10.24

Table 7: The main support technical parameters of the ZZ13000/28/60.

Pattern	Four-column support shield
Height (lowest/highest)	2800/6000 mm
Width (minimum/maximum)	1660/1860 mm
Center distance	1750 mm
Setting load	10128 kN
Working resistance	13000 kN
Specific pressure in front of bottom plate	1.0~3.5 MPa
Support strength	1.24~1.28 MPa
Pumping station pressure	31.5 MPa
Maneuverability pattern	The control of this frame

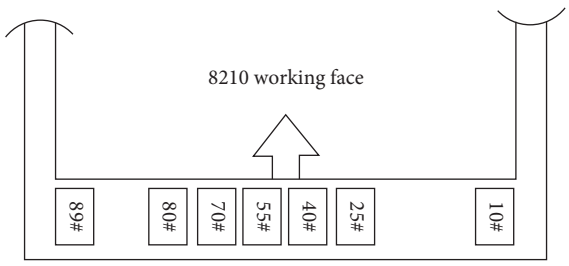

Figure 14: The face pressure observation station layout of No. 8210 working face in large fully mechanized mining face.

face. It shows that, during the normal mining period of the working face, the support ability of the working face is high, which can meet the control requirements of the roof of the coal seam with large mining height, and there is no frame crushing accident in the working face, and the support efficiency is fully exerted.

In summary, the selected ZZ13000/28/60 four-column support shield hydraulic support can meet the roof control requirements of No. 8210 large mining height working face.

5. Conclusions

(1) In the mining process of large mining height working face, the immediate roof of overlying strata exists in the form of combined cantilever beam. With the increase of caving height, the caving gangue gradually fills the goaf space. The bending subsidence of the broken block of the overlying strata of the combined cantilever beam is supported by the caving gangue. At this time, the allowable subsidence space of the goaf exceeds the allowable subsidence of the limit extrusion between the broken blocks of the roof, and the hinged rock-beam structure cannot be formed between the blocks. This part of the rock exists in the form of nonhinged structure. Because the broken block of the nonhinged structure rock is large and the arrangement is regular after collapse, when the rock above the nonhinged structure is broken, the extrusion pressure between the broken blocks is relatively large, and finally the articulated roof structure is formed. The overlying strata roof of fully mechanized mining face with large mining height presents the morphological characteristics of 'combined cantilever beam structure-nonhinged roof structure-hinged roof structure'.

(2) When the working face with large mining height is mined, the overlying strata have a large range of movement and collapse, and the different lithology characteristics of the roof strata lead to the new characteristics of the overlying strata structure. The roof strata between the support and the hinged roof structure cannot be simply regarded as the immediate roof. The interaction system between the support and the surrounding rock is composed of the hinged roof structure-the nonhinged roof structure-the combined cantilever beam structure-the support. The stability of the overburden structure and its influencing factors are studied. According to the principle of the interaction between the support and the surrounding rock, the support resistance should be able to adapt to the change of the instability movement of the overburden structure, bearing the weight of the structure and the additional load generated by the movement, and the calculation formula of the support resistance of the working face is obtained.

(3) The reasonable support resistance of hydraulic support in No. 8210 large mining height working face is determined. The field observation results show that the selected ZZ13000/28/60 four-column support shield hydraulic support can meet the requirements of roof control. During the mining of the working face, there was no support crushing accident in the working face, and the rib spalling of the coal wall was effectively controlled, which ensured the safe mining of the working face with large mining height and achieved significant economic and social benefits.

Data Availability

This is an open access article distributed under the creative commons attribution license, which permits unrestricted use, distribution, and reproduction in any medium, provided the original work is properly cited.

Conflicts of Interest

The authors declare that there are no conflicts of interest regarding the publication of this paper.

Acknowledgments

The work was supported by the National Natural Science Foundation of China (52174138). The authors gratefully acknowledge financial support of the agency mentioned above.

References

[1] G. F. Wang and Y. H. Pang, "Full-mechanized coal mining and caving mining method evaluation and key technology for thick coal seam," *Journal of China Coal Society*, vol. 43, no. 1, pp. 33–42, 2018.

[2] M. G. Qian, P. W. Shi, and J. L. Xu, *Ground Pressure and Strata Control*, China University of Mining and Technology Press, China, 2013.

[3] M. G. Qian, *Key Strata Theory of Strata Control*, China University of Mining and Technology Press, Xuzhou, China, 2013.

[4] J. H. Wang, "Present status and development tendency of fully mechanized coal mining technology and equipment with high cutting height in China," *Coal Science and Technology*, vol. 34, no. 1, pp. 4–7, 2006.

[5] Y. Ning, *Comprehensive Mechanized Mining Technology and Equipment with Large Mining Height in china*, China Coal Industry Publishing House, Beijing, China, 2012.

[6] Y. Q. Xu, *Coal Mining*, China University of Mining and Technology Press, Xuzhou, China, 1999.
[7] F. L. He, M. G. Qian, and C. Y. Liu, *Support Surrounding Rock Support System of High Yield and High Efficiency Working Face*, China University of Mining and Technology Press, Xuzhou, China, 1997.
[8] N. E. Yasitli and B. Unver, "3D numerical modeling of longwall mining with top-coal caving," *International Journal of Rock Mechanics and Mining Sciences*, vol. 42, no. 2, pp. 219–235, 2005.
[9] D. B. Mao and L. J. Kang, "Longwall top coal caving mining with higher mining height and its feasibility," *Coal Mining Technology*, vol. 9, no. 1, pp. 11–14, 2003.
[10] Q. M. Liu and D. B. Mao, "Research on adaptability of full-mechanized caving mining with large," *Mining-height Original Research Article Procedia Engineering*, vol. 26, pp. 652–658, 2011.
[11] P. L. Gong, *Theory of Surrounding Rock and Application Study of the Coal Face with Greater Mining Height*, China Coal Industry Publishing House, Beijing, China, 2006.
[12] P. L. Gong, Z. M. Jin, and H. J. Hao, "Research on stability test for fully mechanized mining support with large mining height," in *Proceedings of the Second International Symposium on Mining Technology*, pp. 246–251, Greenland, 2001.
[13] Q. X. Huang, W. G. Liu, and Y. S. Tian, "Observation on the law of strata behavior in shallow seam and high mining height face," *Ground Pressure and Strata Control*, vol. 20, no. 3, pp. 58-59, 2003.
[14] Z. H. Li, K. Yang, and X. Z. Hua, "Disaster-causing mechanism of instability and 'macroscopic-big-small' structures of overlying strata in longwall mining," *Journal of China Coal Society*, vol. 45, no. S2, pp. 541–550, 2020.
[15] S. H. Yan, X. W. Yin, and H. J. Xu, "Roof structure of short cantilever-articulated rock beam and calculation of support resistance in full-mechanized face with large mining height," *Journal of China Coal Society*, vol. 36, no. 11, pp. 1816–1820, 2011.
[16] J. L. Xu and J. F. Ju, "Structural morphology of key stratum and its influence on strata behaviors in fully mechanized face with super-large mining height," *Chinese Journal of Rock Mechanics and Engineering*, vol. 30, no. 8, pp. 1547–1556, 2011.
[17] G. F. Wang, Y. H. Pang, M. Z. Li, and Y. Ma, "Hydraulic support and coal wall coupling relationship in ultra large height mining face," *Journal of China Coal Society*, vol. 42, no. 2, pp. 518–526, 2017.
[18] J. Ju and J. Xu, "Structural characteristics of key strata and strata behaviour of a fully mechanized longwall face with 7.0m height chocks," *International Journal of Rock Mechanics and Mining Sciences*, vol. 58, pp. 46–54, 2013.
[19] X. W. Yin, "Cutting block structure model of overburden with shallow buried coal seam and ultra-large mining height working face," *Journal of China Coal Society*, vol. 44, no. 7, pp. 1961–1970, 2019.
[20] C. L. Zhang, L. Guo, and M. P. Zhang, "Measurements of working resistance and adaptability analysis of shield in fully mechanized coal face with large mining height and medium buried depth," *Coal Mine Machinery*, vol. 41, no. 6, pp. 68–71, 2020.
[21] F. Q. Qiu, L. Zhu, and W. Z. Gu, "Mining pressure law and working resistance of support in face with large mining height in shallow seam," *Safety in Coal Mines*, vol. 51, no. 11, pp. 243–247, 2020.
[22] H. C. Li, *Similar Simulation Test of Mine Pressure*, China University of Mining and Technology Press, Xuzhou, China, 1988.